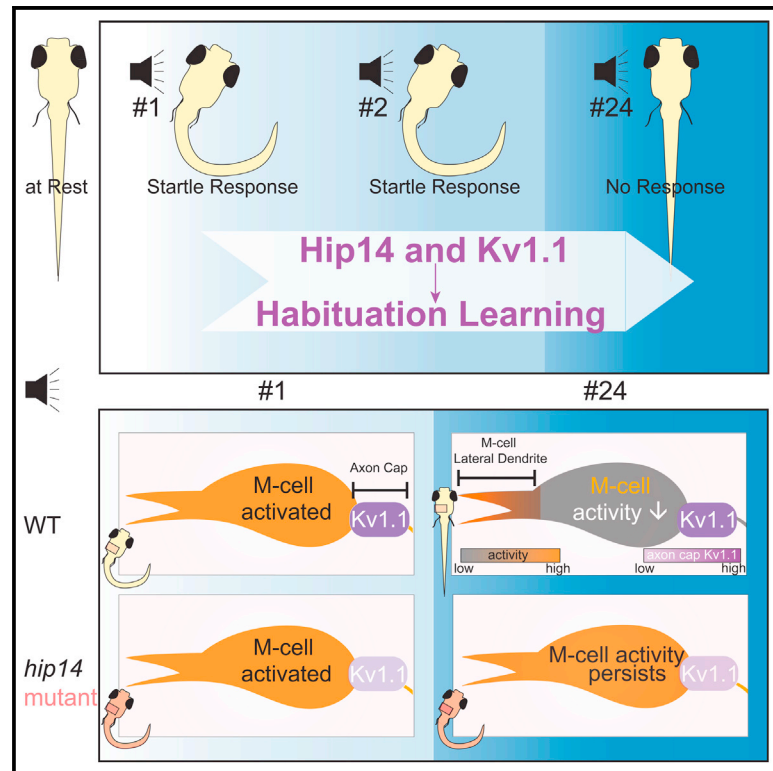


# Acute Regulation of Habituation Learning via Posttranslational Palmitoylation

## Graphical Abstract



## Authors

Jessica C. Nelson, Eric Witze, Zhongming Ma, ..., Owen Randlett, J. Kevin Foskett, Michael Granato

## Correspondence

granatom@penmedicine.upenn.edu

## In Brief

Through a genetic screen, Nelson et al. identify the palmitoyltransferase Hip14 and the voltage-gated K<sup>+</sup> channel subunit Kv1.1 as regulators of habituation learning in zebrafish. They demonstrate that Hip14 acts acutely and regulates synaptic plasticity and propose that Hip14 palmitoylates and thus directs Kv1.1 localization at synaptic sites.

## Highlights

- The palmitoyltransferase Hip14 acutely regulates habituation learning in zebrafish
- Hip14 regulates synaptic depression at an identified hindbrain neuron
- Hip14 regulates learning likely via the VGKC subunit Kv1.1
- Kv1.1 presynaptic localization is regulated by Hip14

Article

# Acute Regulation of Habituation Learning via Posttranslational Palmitoylation

Jessica C. Nelson,<sup>1</sup> Eric Witze,<sup>2</sup> Zhongming Ma,<sup>3</sup> Francesca Ciocco,<sup>4</sup> Abigaile Frerotte,<sup>4</sup> Owen Randlett,<sup>5</sup> J. Kevin Foskett,<sup>3</sup> and Michael Granato<sup>1,6,\*</sup>

<sup>1</sup>Department of Cell and Developmental Biology, Perelman School of Medicine, University of Pennsylvania, 421 Curie Boulevard, Philadelphia, PA 19104, USA

<sup>2</sup>Department of Cancer Biology, Perelman School of Medicine, University of Pennsylvania, 421 Curie Boulevard, Philadelphia, PA 19104, USA

<sup>3</sup>Department of Physiology, Perelman School of Medicine, University of Pennsylvania, 415 Curie Boulevard, Philadelphia, PA 19104, USA

<sup>4</sup>Department of Biology, Haverford College, 370 Lancaster Avenue, Haverford, PA 19041, USA

<sup>5</sup>Institut NeuroMyoGène, Univ Lyon, Université Claude Bernard Lyon 1, CNRS UMR 5310, INSERM U1217, Lyon 69008, France

<sup>6</sup>Lead Contact

\*Correspondence: [granatom@pennmedicine.upenn.edu](mailto:granatom@pennmedicine.upenn.edu)

<https://doi.org/10.1016/j.cub.2020.05.016>

## SUMMARY

Habituation is an adaptive learning process that enables animals to adjust innate behaviors to changes in their environment. Despite its well-documented implications for a wide diversity of behaviors, the molecular and cellular basis of habituation learning is not well understood. Using whole-genome sequencing of zebrafish mutants isolated in an unbiased genetic screen, we identified the palmitoyltransferase Huntingtin interacting protein 14 (Hip14) as a critical regulator of habituation learning. We demonstrate that Hip14 regulates depression of sensory inputs onto an identified hindbrain neuron and provide evidence that Hip14 palmitoylates the Shaker-like K<sup>+</sup> voltage-gated channel subunit (Kv1.1), thereby regulating Kv1.1 subcellular localization. Furthermore, we show that, like for Hip14, loss of Kv1.1 leads to habituation deficits and that Hip14 is dispensable in development and instead acts acutely to promote habituation. Combined, these results uncover a previously unappreciated role for acute posttranslational palmitoylation at defined circuit components to regulate learning.

## INTRODUCTION

Habituation is an evolutionarily conserved non-associative form of learning characterized by a response decrement to repeated stimuli. One of the simplest forms of learning, habituation is defined by ten behavioral characteristics, including spontaneous recovery and sensitivity to dishabituation, which distinguish habituation from other processes, such as sensory adaptation or fatigue [1, 2]. Habituation has been associated with a wide range of behaviors and physiological responses, including feeding and drug seeking [3–5], neuroendocrine responses to stress [6], and mechanosensory [7, 8], olfactory [9], and acoustic startle responses [10]. Moreover, because habituation enables animals to focus selectively on relevant stimuli, it is thought to be a prerequisite for more complex forms of learning [2]. In fact, habituation is impaired in several human disorders that present with more complex cognitive and learning deficits, including autism spectrum disorders, schizophrenia, attention deficit hyperactivity disorder, and Huntington's disease [11], suggesting that some of the molecular, genetic, and circuit mechanisms that act in the context of habituation extend well beyond this form of learning.

Over the past decade, significant progress has been made toward understanding the circuit mechanisms of habituation learning in both vertebrate and invertebrate systems. Studies on sensory habituation in *C. elegans* and *Aplysia* and startle

habituation in zebrafish and rodents have revealed experience-dependent changes in activity at the synapses between sensory afferents and “command” interneurons (neurons that drive a given behavior) during habituation of that behavior [12–17]. Furthermore, genetic screens in *C. elegans* and *Drosophila* have been instrumental in identifying genes that regulate habituation learning [18–28]. Thus, although a picture of habituation in invertebrates is emerging, major questions regarding vertebrate habituation learning remain largely unanswered. For example, does the increased complexity of the vertebrate nervous system dictate additional molecular players and mechanisms that drive habituation learning? Similarly, how many circuit components regulate what we think of as a simple learning process? To address these questions, we previously conducted an unbiased genome-wide screen to identify the first set of mutants with deficits in vertebrate habituation learning [29]. We performed our screen using the larval zebrafish, a system in which habituation learning is observed and adheres to the behavioral characteristics previously described [30]. Here, we report on the molecular identification of two of these mutants and uncover a previously unappreciated role for posttranslational modification by the palmitoyltransferase ZDHHC17/Hip14 (Huntingtin interacting protein 14, which we refer to as Hip14) in regulating habituation. We further identify a previously unknown substrate of Hip14, the Shaker-like K<sup>+</sup> voltage-gated channel subunit (Kv1.1), and show that Kv1.1 regulates learning. Moreover, we find that

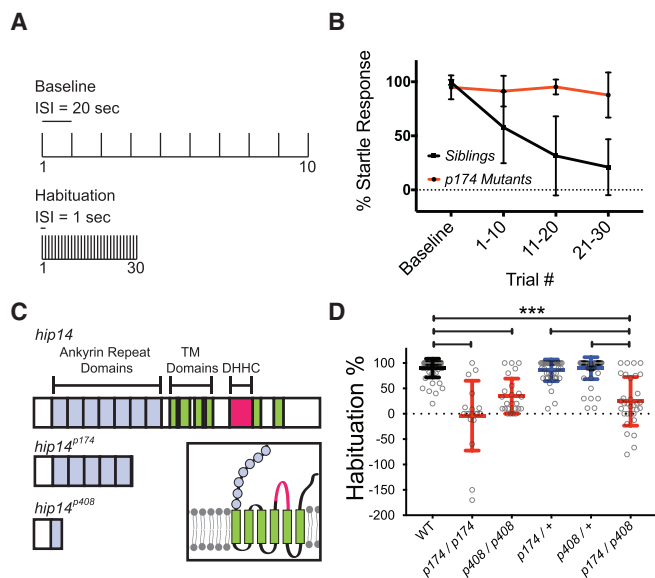


**Figure 1. Hip14 Is Required for Habituation Learning in the Larval Zebrafish**

(A) Acoustic stimulation protocol used to induce habituation learning. Vertical lines indicate acoustic stimuli. 10 stimuli are presented with 20-s ISI to assess baseline startle responsiveness. 30 stimuli are then presented with 1-s ISI to induce habituation learning.

(B) Habituation curves for sibling and *p174* mutant animals. Startle responses are averaged across bins of 10 stimuli (baseline, 10 stimuli at 20 s ISI; 1-10, 1<sup>st</sup> bin of 10 stimuli at 1-s ISI; 11-20, 2<sup>nd</sup> bin of 10 stimuli at 1-s ISI; 21-30, 3<sup>rd</sup> bin of 10 stimuli at 1-s ISI). Mean response frequency within each bin  $\pm$  SD is depicted;  $n \geq 19$  larvae per genotype.

(C) Predicted polypeptide domain structure of Hip14 and Hip14 mutant alleles. Gray indicates ankyrin repeat domains, green indicates transmembrane domains, and pink indicates DHHC catalytic domain. Inset depicts domain conformations.

(D) Complementation testing to confirm mapping of habituation phenotype to *hip14* nonsense mutation. % habituation =  $(1 - [\text{response frequency } 21-30] \div [\text{response frequency baseline}]) \times 100$ . Mean  $\pm$  SD;  $n \geq 18$  larvae per genotype. \*\*\* $p < 0.0001$ ; Kruskal-Wallis test with Dunn's multiple comparisons test.

Hip14 regulates the localization of Kv1.1 to presynaptic terminals onto an identified neuron of the startle habituation circuit and demonstrate that Hip14 promotes habituation learning acutely. Combined, these results support a model by which Hip14 palmitoylates Kv1.1 to ensure its proper localization to presynaptic sites critical for habituation learning. Furthermore, our findings emphasize an emerging role for posttranslational palmitoylation in regulating behavioral plasticity.

## RESULTS

### The Palmitoyltransferase Hip14 Regulates Habituation Learning In Vivo

At 5 days of age, larval zebrafish exhibit robust habituation learning when confronted with a series of high-intensity acoustic stimuli (25.9 dB) as larvae rapidly learn to ignore these apparently innocuous stimuli and cease responding [30, 31]. We have previously uncovered extensive pharmacological conservation of habituation learning between larval zebrafish and adult mammals [30] and

have recently shown that, in zebrafish, habituation is accompanied by increased inhibitory drive combined with decreased excitatory drive converging on an identified hindbrain neuron, the Mauthner (M) cell [14]. To identify genes that regulate habituation learning, we conducted a forward genetic screen using an assay that measures acoustic startle habituation [29]. In this assay, baseline startle responsiveness is first established by presenting larvae with 10 high-intensity acoustic stimuli separated by a 20-s interstimulus interval (ISI) (Figure 1A). To induce habituation learning, 30 additional stimuli are then presented with a 1-s ISI (Figure 1A). Wild-type animals exposed to this protocol rapidly cease responding to acoustic stimuli, exhibiting habituation rates of approximately 80% [29] (Figure 1B). In response to the same stimulation protocol, larvae carrying the *slow learner*<sup>*p174*</sup> mutation exhibit almost no habituation learning (Figure 1B).

To identify the gene disrupted in *slow learner*<sup>*p174*</sup> mutants, we used a previously described whole-genome sequencing (WGS) approach followed by homozygosity mapping [29, 32, 33]. This uncovered a premature stop codon (Y211\*) in the *hip14* gene, encoding a palmitoyltransferase (PAT) that catalyzes the addition of palmitate moieties to cysteine residues of substrate proteins [34]. Like other PAT family members, Hip14 contains transmembrane domains flanking a catalytic palmitoyltransferase (DHHC) domain [34] (Figure 1C). The premature stop codon in *slow learner*<sup>*p174*</sup> mutants is located in the sixth of seven Ankyrin repeat domains and thus precedes the catalytic palmitoyltransferase domain. To confirm that mutations in *hip14* indeed cause the observed habituation phenotype, we generated a second allele, *hip14*<sup>*p408*</sup> using CRISPR-Cas9 genome-editing techniques [35, 36]. This allele truncates the protein after amino acid 67 (Figure 1C). Animals heterozygous for either *hip14*<sup>*p408*</sup> or the original allele, *hip14*<sup>*p174*</sup>, show normal rates of habituation, although larvae carrying a combination of both mutant alleles (*hip14*<sup>*p408/p174*</sup>) fail to habituate at rates comparable to larvae homozygous for *hip14*<sup>*p174*</sup> or *p408* (Kruskal-Wallis test with Dunn's multiple comparisons test = not significant [NS]). Together, these data establish that mutations in *hip14* cause habituation deficits (Figure 1D) and demonstrate that the palmitoyltransferase Hip14 regulates habituation learning.

### Hip14 Regulates Synaptic Depression of Neurons of the Acoustic Startle Circuit

The neuronal circuits that govern acoustic startle behavior in the larval zebrafish are well defined, and multiple circuit components are analogous to those described in other vertebrates [37–40]. As in mammals, acoustic stimuli are detected by hair cells within the inner ear and conveyed via the auditory (VIIIth) cranial nerve to the hindbrain. There, VIIIth nerve axons form synapses onto the lateral dendrite of the M cell, which is the zebrafish analog of giant caudal pontine reticular nucleus (PnC) neurons. When inputs are sufficient to drive the M cell to fire an action potential, M cell axons directly activate spinal motoneurons to initiate execution of the startle response (Figure 2A) [40–42]. To examine whether Hip14 regulates habituation at the level of the M cell, we performed Ca<sup>2+</sup> imaging of M cell activity in *hip14* mutants. We have previously established an assay to simultaneously monitor M cell Ca<sup>2+</sup> transients and startle behavior in head-fixed zebrafish larvae [14]. Using this assay, we have shown that acoustic inputs above 12 dB trigger Ca<sup>2+</sup> signals that spread

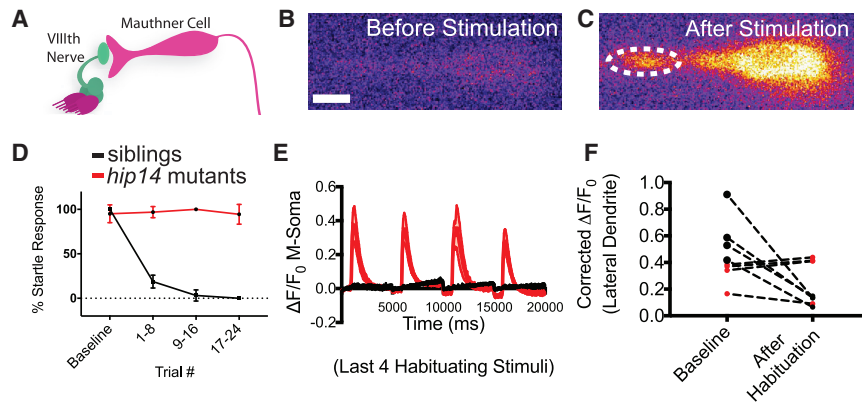


**Figure 2. *hip14* Mutants Fail to Exhibit Synaptic Depression at the Mauthner Lateral Dendrite**

(A) Diagram of auditory nerve inputs onto the Mauthner cell. The lateral dendrite, the site of these inputs, is one known locus for acoustic startle habituation.

(B and C) Single frames showing GCaMP6s expressed in the Mauthner cell (B) in an unstimulated animal and (C) following a high-intensity acoustic stimulus.

(D) Habituation curves for head-embedded *hip14* mutant and sibling animals. Baseline, average of 5 responses at 2-min ISI; 1-8, 1<sup>st</sup> bin of 8 responses at 5-s ISI; 9-16, 2<sup>nd</sup> bin of 8 responses at 5-s ISI; 17-24, 3<sup>rd</sup> bin of 8 responses at 5-s ISI. Mean  $\pm$  SD;  $n = 4$  larvae per genotype.

(E) Final 4 Mauthner soma responses (stimuli no. 21-24). By this point, sibling animals are fully habituated and no longer perform startle responses. Concomitantly,  $Ca^{2+}$  activity in the Mauthner soma has subsided. *hip14* mutants show no/minimal behavioral habituation and exhibit robust  $Ca^{2+}$  responses in the soma. Mean  $\pm$  shading indicates SEM;  $n = 4$  larvae per genotype.

(F) Lateral dendrite responses before and after habituation in sibling and *hip14* mutant animals. Note the significant reduction in lateral dendrite  $Ca^{2+}$  activity in siblings (black), whereas *hip14* mutants show little/no such reduction (red). Mean lateral dendrite response;  $n = 4$  larvae per genotype. Mutant lateral dendrite responses undergo significantly less depression than wild-type (WT) responses; unpaired t test; habituated responses  $\div$  baseline responses;  $p = 0.0021$ . Scale bar, 10  $\mu$ m. See also Figure S1.

from the lateral dendrite to the M cell soma to elicit tail deflections with kinematic parameters characteristic of the acoustic startle response (Figures 2B-2D and S1) [14]. In wild-type larvae, repeated acoustic stimuli induce rapid habituation of acoustic startle behaviors (tail deflections), accompanied by reduced M cell  $Ca^{2+}$  signals (Figures 2D, 2E, and S1). In contrast, *hip14* mutants exposed to the same stimuli continue to display robust  $Ca^{2+}$  transients and their startle responses fail to habituate (Figures 2D, 2E, and S1). Moreover, unlike their sibling counterparts, *hip14* mutant M cell dendrites exhibit little to no synaptic depression (Figures 2F and S1). Combined, these results demonstrate that, during habituation learning, Hip14 regulates synaptic depression upstream of or at the level of the M cell lateral dendrite.

### Hip14 Acts Independently of Previously Identified Regulators of Habituation Learning

To understand how *hip14* promotes habituation learning at the molecular level, we wanted to identify learning relevant Hip14 substrates. Hip14 was originally isolated based on molecular interactions with the Huntington's disease-associated Huntingtin protein [43]. Since its discovery, hundreds of potential substrates of Hip14 palmitoylation and interacting partners have been reported [34, 44-52]. Interestingly, several proteins shown to interact with Hip14 are components of genetic pathways we previously implicated in habituation learning in the larval zebrafish. First, Hip14 interacts with phosphatidylinositol 3-kinase (PI3K) and AKT activators that we previously demonstrated promote acoustic startle habituation downstream of the PAPP-AA/insulin growth factor receptor (IGF1R) signaling pathway (Figure 3A) [29, 45]. Second, Hip14 also interacts with PDE4, which we showed acts downstream of the *neurofibromatosis-1* (*nf1*) gene to regulate visual habituation learning (Figure 3A) [45, 53]. Importantly, habituation deficits in zebrafish *papp-aa* or *nf1* mutants can be restored by pharmacological manipulation of PI3K, AKT, cyclic AMP (cAMP), and RAS signaling [29, 53]. To determine whether

these intracellular signaling pathways also function downstream of Hip14, we repeated the same pharmacological manipulations with *hip14* mutants. We found that manipulating PI3K, AKT, cAMP, and RAS signaling in *hip14* mutants failed to restore habituation learning (Figures 3B-3D and S2), strongly suggesting that Hip14 acts independently of the PAPP-AA/IGF1R and NF1 learning pathways.

### The Shaker-like Voltage-Gated K<sup>+</sup> Channel Subunit Kv1.1 Regulates Habituation Learning

Given the evidence that Hip14 likely acts independently of some of the known learning-relevant signaling pathways, we turned to our forward genetic screen, reasoning that other mutants with habituation deficits might represent potential Hip14 interaction partners or even substrates relevant in the context of learning. In particular, *fool-me-twice*<sup>D181</sup> mutants show strong deficits in habituation learning similar to those observed in *hip14* mutants (Figure 4A). Whole-genome sequencing of *fool-me-twice*<sup>D181</sup> mutants revealed a missense mutation leading to an amino acid substitution (N250K) in the coding sequence for *kcna1a*, which encodes the Shaker-like voltage-gated K<sup>+</sup> channel subunit Kv1.1 (Figures 4B and 4C). Shaker-like K<sup>+</sup> channels are critical regulators of neuronal activity; in mutants lacking Shaker and Shaker-like K<sup>+</sup> channels, neuronal repolarization is delayed [54], neurons are hyperexcitable [55] and release more quanta upon stimulation [56], and animals display behavioral hyperexcitability and seizure-like behaviors [57, 58].

The lysine residue mutated in *fool-me-twice*<sup>D181</sup> mutants, N250, is highly conserved across species. Substitution of lysine for asparagine at this precise residue occurs in human patients with the disorder familial paroxysmal kinesigenic dyskinesia [59]. Together, these data suggest that the N250K substitution in *fool-me-twice*<sup>D181</sup> mutants might affect Kv1.1 function (Figure 4D). To determine whether the Kv1.1<sup>N250K</sup> substitution alters channel properties, we performed whole-cell current recordings in N2a cells expressing wild-type and mutant versions of Kv1.1

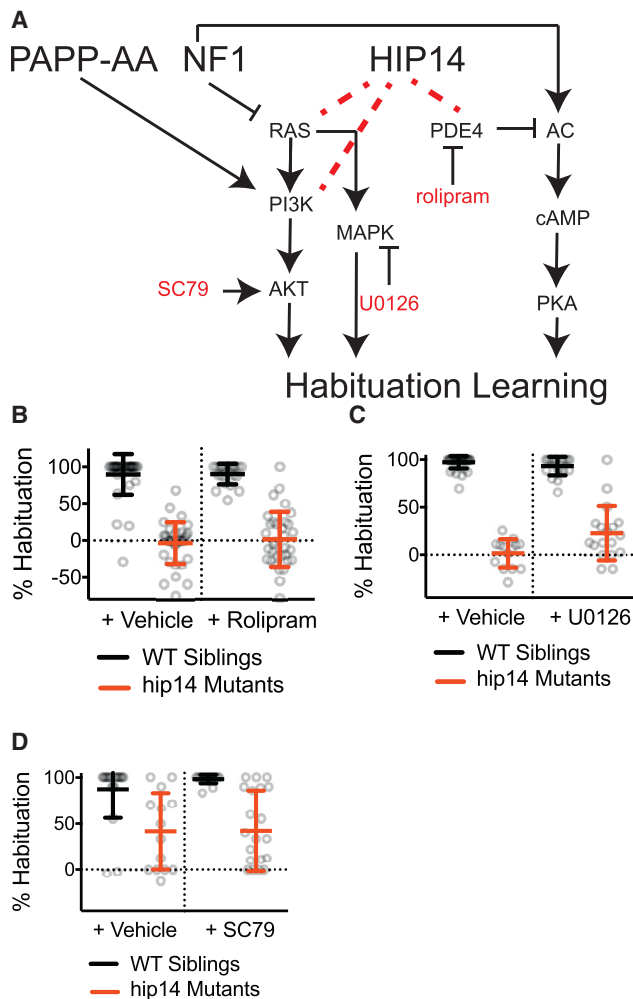


**Figure 3. Hip14 Acts Independently of Previously Established Habituation Pathways**

(A) Pathway diagram indicating cellular mechanisms of action for PAPP-AA and NF1. Red text denotes drugs that impinge on individual pathway elements. Dotted lines indicate biochemical interactions between proteins that may or may not play a functional role in regulating habituation learning.

(B–D) Habituation rates in *hip14* mutants and sibling larvae are unaffected by pharmacological manipulation of known habituation pathways: (B) 10  $\mu$ M rolipram (or DMSO control) applied 30 min prior to and throughout behavior testing. (C) 1  $\mu$ M U0126 (or DMSO control) applied 30 min prior to and throughout behavior testing. (D) 1  $\mu$ M SC-79 (or DMSO control) applied from 3 dpf to 5 dpf and throughout behavior testing. Mean  $\pm$  SD; differences between mutants treated with vehicle compared to drug are not significant according to Kruskal-Wallis test with Dunn's multiple comparisons test.  $n \geq 14$  larvae for each condition. See also Figure S2.

(as well as vector only control; Figure 4E). To account for differences in cell size across conditions, whole-cell currents recorded under voltage clamp were normalized to whole-cell capacitance. These experiments revealed that the Kv1.1<sup>N250K</sup> substitution completely abolishes conductance, consistent with the hypothesis that the habituation deficit observed in *fool-me-twice*<sup>p181</sup> mutant zebrafish is caused by a nonfunctional Kv1.1 (Figures 4F–4H). Finally, we used CRISPR-Cas9 genome

editing to generate a zebrafish line carrying a premature stop codon in *kcna1a* (*p410*). Complementation analysis with the original *kcna1a*<sup>p181</sup> allele confirmed that loss-of-function mutations in *kcna1a* cause deficits in habituation learning (Figure 4I).

### Presynaptic Kv1.1 Localization Requires Hip14-Dependent Palmitoylation

Both Hip14 and Kv1.1 regulate habituation learning, and previous studies have revealed that palmitoylation of Kv1.1 by an as-yet-undefined palmitoyltransferase or palmitoyltransferases regulates voltage sensing [60]. Therefore, we hypothesized that Hip14 may act in part by palmitoylating Kv1.1. To test this hypothesis, we employed the acyl biotin exchange (ABE) assay [61], which can be used to determine whether a given enzyme palmitoylates a particular substrate. In this assay, palmitoyltransferases and putative substrates are co-expressed in cultured cells and palmitoylated cysteines are subsequently labeled. We first validated our system using the well-characterized Hip14 substrate, SNAP-25 [34], and an independent palmitoyltransferase DHHC7 (Figure S3). Having validated the ABE assay, we co-expressed FLAG-tagged recombinant Kv1.1 and hemagglutinin (HA)-tagged recombinant Hip14 in HEK cells. We found that, in the absence of Hip14, Kv1.1 is not palmitoylated above background levels (Figure 5A). In contrast, Kv1.1 was robustly palmitoylated in HEK cells co-expressing Hip14, demonstrating that Hip14 can palmitoylate Kv1.1 (Figure 5A). To demonstrate that Hip14 catalytic activity is indeed required for Kv1.1 palmitoylation, we generated a catalytically inactive version of Hip14, Hip14-DHHS (Hip14<sup>C455S</sup>), by substituting a serine for the cysteine in the DHHC domain critical for Hip14 catalytic activity. In contrast to co-expression with wild-type Hip14, co-expression of Hip14-DHHS with Kv1.1 dramatically reduced levels of palmitoylated Kv1.1 (Figure 5A).

In the human Kv1.1 channel, cysteine 243 has been identified as a critical palmitoylation site, although other sites are likely palmitoylated at a low level, given the residual palmitoylation observed in C243A point mutant proteins [60]. We wondered whether Hip14 might palmitoylate the corresponding cysteine (C238) in the zebrafish Kv1.1 sequence. As in the case of the human protein, we observed a strong decrement in palmitoylation of the C238A mutant version of Kv1.1, indicating that this particular cysteine is critical for Hip14-dependent palmitoylation of Kv1.1 (Figure 5B). Finally, we found that co-expression of wild-type Hip14 with the Kv1.1<sup>N250K</sup> mutant isolated in the genetic screen produced a marked reduction in palmitoylated Kv1.1 (Figure 5B). Together, these data indicate that Hip14 can act as a Kv1.1 palmitoyltransferase, suggesting that Hip14 may promote habituation learning through Kv1.1.

Posttranslational palmitoylation is known to regulate substrate function as well as substrate localization [62]. Therefore, we hypothesized that Hip14-dependent palmitoylation might regulate Kv1.1 protein localization. To test this *in vivo*, we turned to immunohistochemistry and examined the localization of Kv1.1 in *hip14* sibling and mutant animals. Previous work in 3-day-old zebrafish larvae has shown that Kv1.1 is expressed throughout the hindbrain, including the M cell soma, and that *kcna1a* mRNA is present in the M cell as late as 5 days post-fertilization [63, 64]. We find that, in 5-day-old sibling animals, Kv1.1 protein expression persists throughout the CNS, including in hindbrain neurons

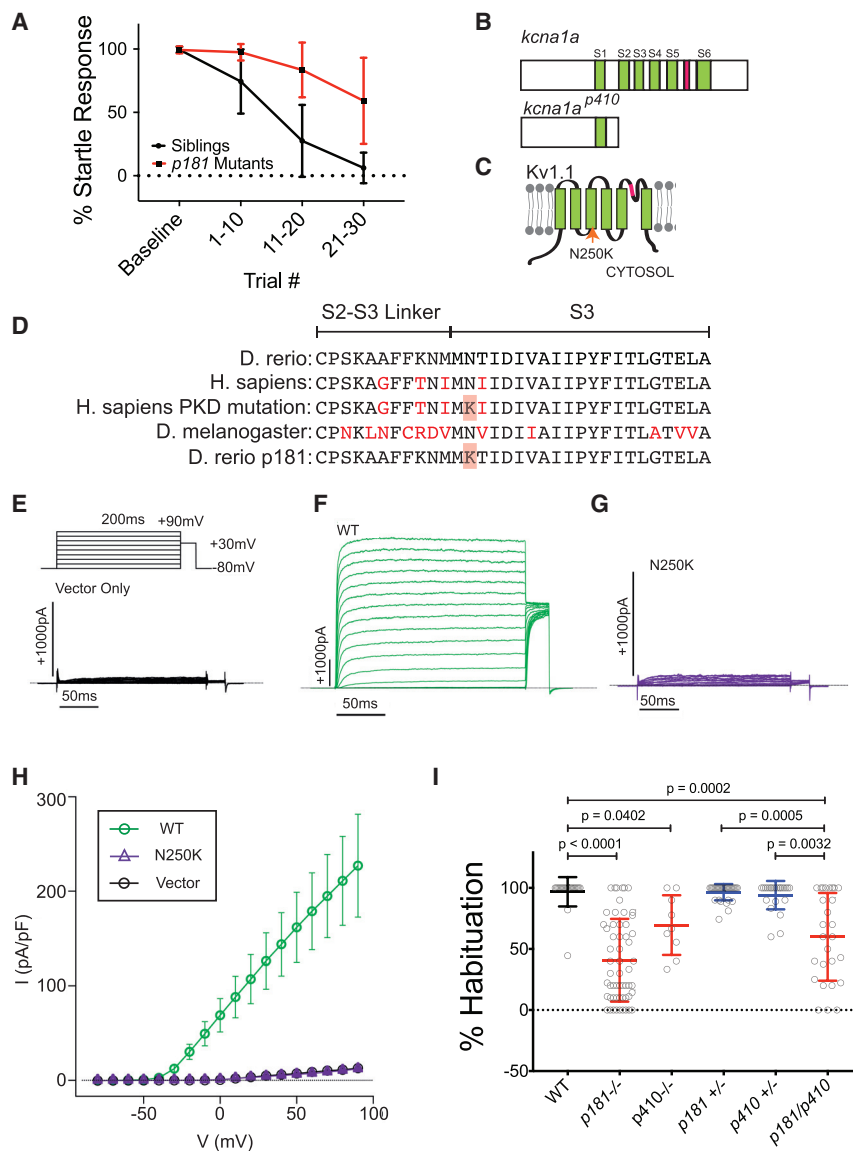


**Figure 4. Kv1.1 Is Required for Habituation Learning in the Larval Zebrafish**

(A) Habituation curves for *p181* mutant animals and siblings. Startle responses are averaged across bins of 10 stimuli (as in Figure 1A). Mean response frequency within each bin  $\pm$  SD is depicted.  $n \geq 57$  per genotype.

(B and C) Predicted polypeptide (B) domain structure of *kcna1a* mutant alleles and (C) domain structure of Kv1.1. Transmembrane domains are in green, and pore helix domain is shown in pink. Orange arrow indicates N250K missense mutation identified in Kv1.1 encoded by *kcna1a*<sup>p181</sup>.

(D) Alignment demonstrating strong conservation of Kv1.1 S2-S3 linker and S3 domain sequences. Note that the N250K missense mutation identified in our screen is equivalent to the N255K missense mutation associated with human PKD disease.

(E-G) Representative whole-cell  $K^+$  family currents evoked by 200-ms voltage pulses from  $-80$  to  $+90$  mV in 10-mV increments from a holding potential of  $-80$  mV as in Figure 1E, top, in N2a cells transfected with (E) vector only (control); cell capacitance of 15.5 pF, (F) wild-type Kv1.1; cell capacitance of 18.2 pF, and (G) Kv1.1<sup>N250K</sup>; cell capacitance of 14.9 pF. For details of solutions, see the STAR Methods section. Dashed lines indicate 0-current level.

(H) Steady-state current-voltage (I-V) relations for vector (control), wild-type Kv1.1, and Kv1.1<sup>N250K</sup>, obtained by measurements of the currents at the end of 200-ms pulses, normalized by the cell capacitance, e.g., the normalized currents at  $+90$  mV are  $226.9 \pm 54.5$  (pA/pF) for wild type ( $n = 6$ ),  $12.8 \pm 1.0$  (pA/pF) for Kv1.1<sup>N250K</sup> ( $n = 7$ ), and  $11.2 \pm 1.2$  (pA/pF) for vector ( $n = 5$ ). Two-tailed Student's unpaired t test:  $p = 0.003$ ,  $t_9 = 3.89$  for wild type and  $p = 0.315$ ,  $t_{10} = 1.06$  for Kv1.1<sup>N250K</sup>, compared to vector, indicating Kv1.1<sup>N250K</sup> is a nonfunctional channel. The cells used in these measurements had the whole-cell capacitance of  $14.8 \pm 1.6$  (pF;  $n = 5$ ) for vector,  $15.4 \pm 0.8$  (pF;  $n = 6$ ) for wild type, and  $14.9 \pm 1.3$  (pF;  $n = 7$ ) for Kv1.1<sup>N250K</sup>, respectively.

(I) Complementation testing to confirm mapping of habituation phenotype to *kcna1a* missense mutation. Mean  $\pm$  SD;  $n \geq 9$  larvae per genotype.  $p$  values for Kruskal-Wallis test with Dunn's multiple comparisons test are indicated.

of the startle circuit, yet only weakly localizes to the M cell soma or lateral dendrite. Instead, Kv1.1 strongly localizes to a structure termed the axon cap (Figures 5C and 5D), which is largely composed of dense synaptic terminals from feedforward spiral fiber neurons that wrap around the axon initial segment of the M cell axon [65, 66]. Given the low Kv1.1 levels at the lateral dendrite and the strong accumulation of Kv1.1 in the axon cap, we selected the axon cap to determine whether and to what extent Kv1.1 localization requires *hip14*. Analysis of *hip14* mutants revealed a significant reduction of Kv1.1 protein localization at the axon cap (Figures 5C, 5D, and S3). Together, these biochemical and immunohistochemical results identify Kv1.1 as a putative substrate of Hip14 and support a model in which Hip14 regulates Kv1.1 localization to presynaptic terminals of the acoustic startle circuit to promote habituation learning.

### Hip14 Acts Acutely to Regulate Habituation Learning

Palmitoylation has previously been shown to function during development in the establishment of neural connectivity, as well as acutely in response to neural activity [62]. In neurons, palmitoylation can occur in both somatic Golgi, as well as in axons and dendrites [62]. Given that Hip14 has been observed in axons and presynaptic sites [49, 67], it is conceivable that Hip14 promotes habituation learning either during development by helping to establish the habituation circuitry or acutely, for example, at synapses by dynamically palmitoylating effector proteins. Development of the major components of the acoustic startle circuit is well defined and largely occurs between 24 and 96 h post-fertilization (hpf) [68]. Larvae perform acoustic startles and are capable of habituation learning at 96 hpf, indicating that the circuit elements required for habituation are in place by this time (Figure 6A). To distinguish between developmental versus acute

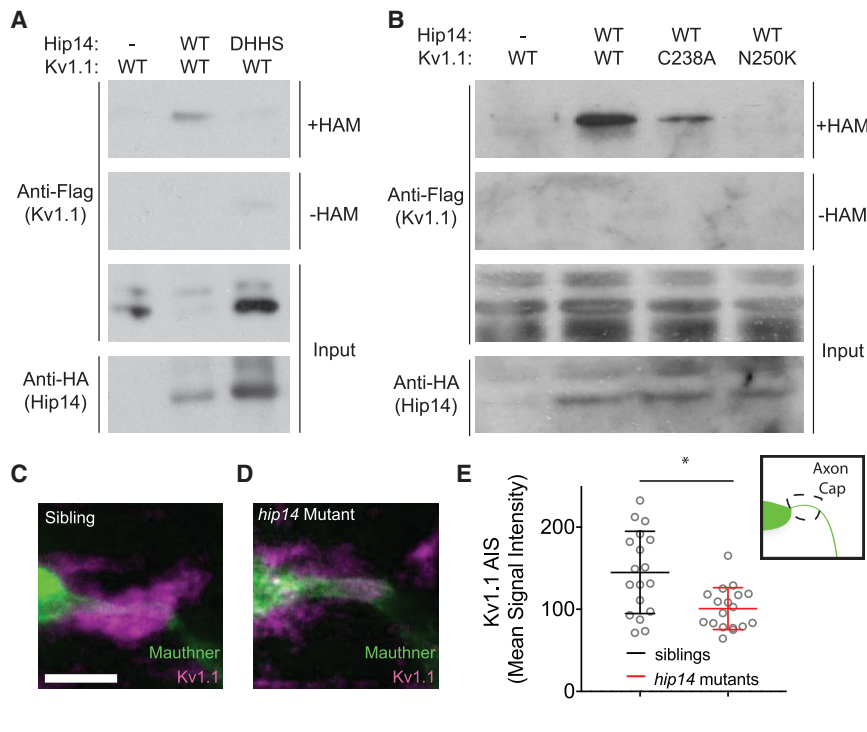


**Figure 5. Hip14 Palmitoylates Kv1.1 and Regulates Its Localization In Vivo**

(A and B) Acyl biotin exchange assays, in which Kv1.1-FLAG  $\pm$  Hip14-HA are transfected into HEK cells. Only in the presence of WT Hip14-HA, WT Kv1.1-FLAG, and hydroxylamine (+HAM) does robust palmitoylation of Kv1.1-FLAG occur. Samples without hydroxylamine (–HAM) are negative controls for the ABE reactions. (A) Mutation of the Hip14 DHHC domain disrupts Kv1.1 palmitoylation. (B) Mutations in Kv1.1 disrupt its palmitoylation.

(C) Immunohistochemical labeling of the Mauthner cell (green) and Kv1.1 (magenta) in *gffDMC130a; uas:gap43:citrine* sibling, using chicken anti-GFP and rabbit anti-Kv1.1 antibodies. Note the bright localization of Kv1.1 to the axon cap: synaptic inputs from spiral fiber neurons onto Mauthner cell AIS are shown.

(D) Immunohistochemical labeling of a *hip14* mutant animal as in (C). Note the reduction in Kv1.1 signal at the axon cap.

(E) Quantification of Kv1.1 signal in mutants as compared to WT. Mean signal intensity, pixel intensity for axon cap region of interest (inset) divided by axon cap area. Unpaired t test;  $p = 0.0021$ .

Scale bar, 10  $\mu$ m. Mean  $\pm$  SD; n = 18 axon caps per genotype (n  $\leq$  2 axon caps per animal). See also Figure S3.

regulation of learning, we generated a zebrafish line stably expressing a transgene composed of the *hip14* coding sequence under the control of the *hsp70* heat-shock-activated promoter. We found that inducing *hip14* expression from the *hsp70* heat-shock promoter by shifting larvae to 37°C at 4 days post-fertilization (dpf) (after the startle circuit becomes functional) was sufficient to fully rescue learning deficits in *hip14* mutants (Figure 6B). This demonstrates that the *hsp70:hip14* transgene is functional and rules out a role for *hip14* in early development. Importantly, the transgene had no effect on habituation learning under normal raising conditions (28°C), indicating that transgenic *hip14* expression is dependent on heat-shock induction (Figure 6C). In order to test whether Hip14 acts acutely, we shifted larvae to 37°C at 5 dpf, only 3 h before behavior testing. We found that this acute induction of Hip14 expression was sufficient to restore habituation learning in mutants (Figures 6D and S4). The same manipulation was also sufficient to restore startle threshold phenotypes observed in *hip14* mutants (Figure S4). On the other hand, restoration of Hip14 expression either at 96 or 117 h failed to rescue spontaneous movement deficits. Similarly, we could not detect restoration of Kv1.1 localization to the axon cap in mutant animals in response to either the 96- or 117-h heat-shock manipulations (Figure S4). Nonetheless, full restoration of learning deficits in response to these manipulations strongly indicates that Hip14 acts after the development of startle circuit elements required for habituation, supporting a model by which Hip14-dependent palmitoylation of learning-relevant substrates acutely promotes habituation learning.

## DISCUSSION

Habituation learning was initially described in the context of reflex responses [1, 8]; however, there has since been broad

recognition that habituation learning is a widespread mechanism associated with and to some degree a prerequisite for more complex cognitive processes and behaviors [3–6, 11]. Although our understanding of habituation learning both at the molecular and cellular level has been informed predominantly by molecular-genetic studies in invertebrates [18–28], whether and how additional genetic and circuit mechanisms regulate vertebrate habituation learning has remained largely unclear. Here, we describe a previously unappreciated role for the palmitoyltransferase Hip14 in regulating habituation learning. Moreover, we identify the Shaker-like channel subunit Kv1.1 as a putative Hip14 substrate that also regulates learning and demonstrate that Hip14 acts to properly target Kv1.1 channel subunits to presynaptic sites. Finally, we show that Hip14 acts acutely to promote habituation learning. Combined, these results provide compelling evidence for Hip14-dependent palmitoylation as a dynamic regulator of habituation at a specific learning-relevant synapse.

Palmitoylation has received considerable attention as a post-translational modification regulating synaptic plasticity [62, 69–73]. Furthermore, Hip14 plays important roles in the nervous systems of invertebrates and vertebrates. For example, *Drosophila* Hip14 localizes to presynaptic terminals, where it regulates their development [67]. In rodents, *hip14* is implicated in a variety of behaviors [46, 74, 75], yet the relevant substrates and whether *hip14* acts acutely or as a regulator of neuronal development or maintenance in these contexts has not been examined. Thus, our findings that Hip14 acts acutely during learning or just before to “prime” learning-relevant synapses reveal a previously unappreciated dynamic role for Hip14-dependent palmitoylation. It is important to note that Hip14 is fairly unique among palmitoyltransferases in that its N terminus is composed of ankyrin-repeat domains that may confer additional functions

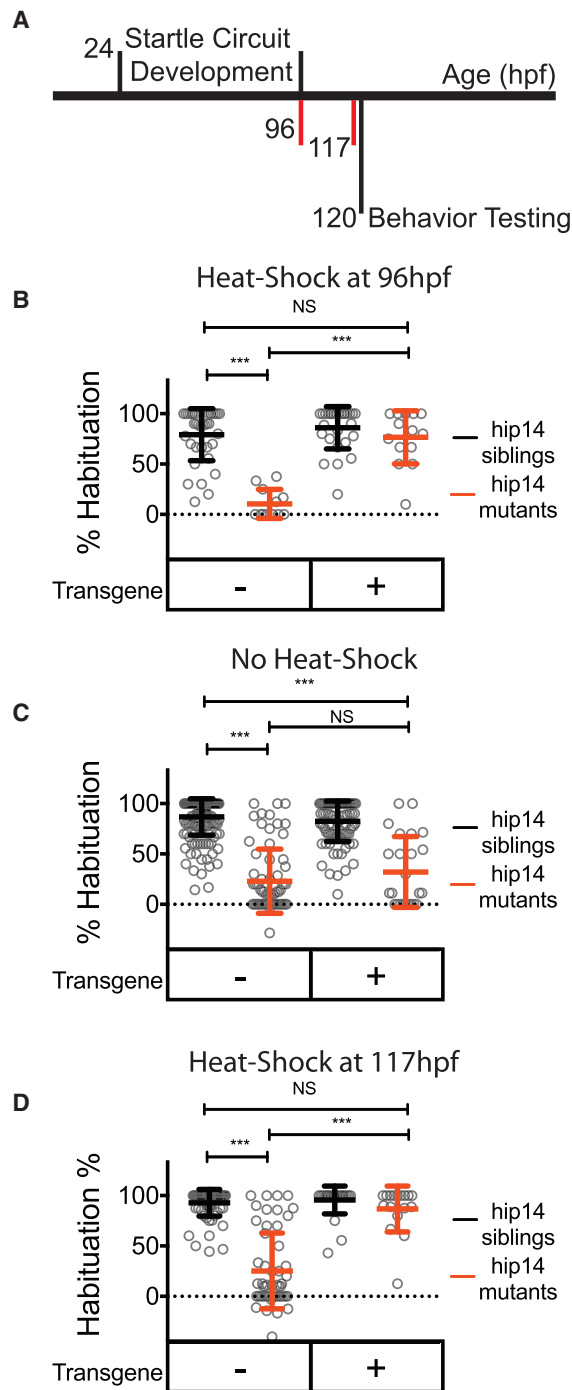


**Figure 6. Hip14 Acutely Regulates Habituation Learning**

(A) Timeline depicting startle circuit development and heat shock timing. Numbers indicate hours post-fertilization. Red vertical lines indicate start times for heat-shock (96 h in B and 117 h in D). (B) Rates of habituation in animals heat-shocked at 37°C at 96 h post-fertilization (4 dpf). (C) Rates of habituation in animals without heat-shock. (D) Rates of habituation in animals heat-shocked at 37°C at 117 h post-fertilization (5 dpf).

In (B)–(D), testing is always performed at 120 hpf (5 dpf). Transgene, *hsp70:hip14;p2a:mKate*; mean ± SD; n ≥ 12 per genotype; \*\*\*p < 0.0001 One-

beyond palmitoylation. This raises the intriguing possibility that Hip14 may act in part through palmitoylation-independent mechanisms to localize Kv1.1 protein, and future experiments are required to test this idea. Similarly, as palmitoylation is dynamically regulated, it will be interesting to determine whether dynamic regulation of protein de-palmitoylation is implicated in learning.

We have previously reported that, in addition to decrements in habituation learning, the *hip14<sup>P174</sup>* mutation results in acoustic hypersensitivity and reduced spontaneous locomotion. Given the ability to acutely restore habituation learning and hypersensitivity, but not spontaneous locomotion deficits (Figure S4), we hypothesize that learning deficits in *hip14* mutants are independent of locomotor changes. These data are consistent with results from our genetic screen demonstrating that, although phenotypes relating to startle sensitivity, habituation, and spontaneous locomotion can occur together as the result of a single mutation, deficits in each of these processes are also observed in isolation [29, 33]. Future studies are required to dissect the relationship between innate regulation of startle sensitivity and acute modulation of sensitivity, as in the case of habituation.

Our results also suggest an evolutionarily conserved role for Kv1.1, a Shaker-like channel subunit identified in *Drosophila* for opposing roles in enhancing and suppressing habituation in different contexts [76, 77]. Importantly, the identical amino acid substitution Kv1.1<sup>N250K</sup> recovered in our genetic screen has previously been identified in humans (Kv1.1<sup>N255K</sup>) as associated with the movement disorder, familial paroxysmal kinesigenic dyskinesia [59]. Previous work indicates that this mutation does not affect membrane expression of Kv1.1 but strongly reduces channel currents [59], consistent with our findings that currents are abolished in cells expressing the Kv1.1<sup>N250K</sup> allele (Figure 4G). We demonstrate that this mutation also affects Hip14-dependent Kv1.1 palmitoylation. Given the importance of palmitoylation for Kv1.1 gating and function [60], we propose that disrupted palmitoylation may represent one way in which this *kcnk1a* mutation leads to disrupted channel function and voltage gating. Indeed, multiple lines of evidence support the hypothesis that Hip14 regulates Kv1.1 localization and function through palmitoylation. First, mutants for each gene show a similar behavioral phenotype. Second, *in vitro*, Hip14 palmitoylates Kv1.1 but fails to palmitoylate the learning-defective point mutant version of Kv1.1. Lastly, *in vivo*, Hip14 is required for Kv1.1 protein localization to defined presynaptic sites.

Although we were able to rescue habituation phenotypes observed in *hip14* mutants, we were not able to detect restoration of Kv1.1 localization to the axon cap in response to heat-shock restoration of Hip14 expression. This dissociation between Kv1.1 localization and behavioral phenotypes could indicate an inability of our immunostaining assay to detect low levels of Kv1.1 localization sufficient to restore learning. Indeed, heat-shock alone at 117 h eliminated the Kv1.1 localization deficit in *hip14* mutants, suggesting a potentially confounding effect of this manipulation on our ability to detect the Kv1.1 localization phenotype. It is also possible that learning phenotypes are driven

way ANOVA with Tukey's test for multiple comparisons; NS, not significant. See also Figure S4.

by deficits in Kv1.1 localization elsewhere in the brain. Alternatively, heat-shock restoration of *hip14*-dependent learning phenotypes might act through Kv1.1-independent palmitoylation substrates. Future studies are required to dissect the precise locus of action for Hip14 and Kv1.1 and to identify all of the substrates that might function downstream of Hip14 to regulate learning.

Although it is viewed as a simple form of learning, previous work has suggested that multiple and potentially intersecting pathways drive habituation. We have previously shown that the M cell lateral dendrite undergoes synaptic depression during habituation learning [14]. Here, we demonstrate that depression at the lateral dendrite is disrupted in Hip14 mutants, consistent with a role for Hip14 and Kv1.1 at this defined circuit locus. It is possible that, to promote habituation learning, Hip14 and Kv1.1 are additionally engaged at other neural circuit loci, including at the M cell axon cap, where synaptic inputs from spiral fiber neurons terminate on the M cell AIS and where we observe a requirement for Hip14 to localize Kv1.1 to terminals (Figures 5C and 5D). Additional experiments are required to determine the precise cell type(s) and synapse(s) at which Hip14/Kv1.1 function to promote acoustic startle habituation in zebrafish. Similarly, it will be interesting to determine whether other molecular regulators of habituation identified in the zebrafish, such as Ap2s1-dependent endocytosis [29, 32], glutamate signaling [30], NF1 signaling through cAMP and Ras [53], or insulin growth factor signaling through PI3K and AKT [29], function at the same or different circuit loci and on the same or different timescales. Together with the results presented here, understanding how these pathways fit together and how and whether these molecular pathways are influenced by neuronal activity will provide an integrated perspective on how vertebrate habituation learning occurs *in vivo*.

## STAR★METHODS

Detailed methods are provided in the online version of this paper and include the following:

- **KEY RESOURCES TABLE**
- **RESOURCE AVAILABILITY**
  - Lead Contact
  - Materials Availability
  - Data and Code Availability
- **EXPERIMENTAL MODEL AND SUBJECT DETAILS**
- **METHOD DETAILS**
  - Behavior Testing
  - WGS and Molecular Cloning of *hip14* and *kcna1a*
  - Ca<sup>2+</sup> Imaging
  - Pharmacology
  - Electrophysiology in N2a cells
  - ABE Palmitoylation Assays
  - Immunohistochemistry
  - Heat Shock-Induced *hip14* Rescue
- **QUANTIFICATION AND STATISTICAL ANALYSIS**

## SUPPLEMENTAL INFORMATION

Supplemental Information can be found online at <https://doi.org/10.1016/j.cub.2020.05.016>.

## ACKNOWLEDGMENTS

The authors would like to thank Drs. Kawakami and Raper for the gal4 driver *Tg:GFFDMC130a* and *UAS-GAP43-Citrine* fish lines, respectively. The authors would also like to thank Dr. Schoppik for the gal4 driver *Tg(6.7FRhcrTR:gal4VP16)* and *Tg:UAS:GCaMP5* fish lines. The authors would also like to acknowledge the Cell and Developmental Biology Microscopy Core and the University of Pennsylvania Next-Generation Sequencing Core. We also thank the Granato lab members, as well as Drs. Marc Wolman, Roshan Jain, and Kurt Marsden for technical advice and feedback on the manuscript. This work was supported by grants to M.G. (NIH R01 MH109498), E.W. (NIH R01 CA181633 and ACS RSG-15-027-01), J.C.N. (1K99NS111736-01A1), and J.K.F. and Z.M. (NIH R01 DC012538). J.C.N. was supported by an NRSA: 5F32MH107139. F.C. was supported by the Haverford Velay Scholars program. A.F. was supported by the Haverford KINSC Summer Scholars program.

## AUTHOR CONTRIBUTIONS

Conceptualization, J.C.N. and M.G.; Investigation, J.C.N., E.W., F.C., A.F., and Z.M.; Formal Analysis, J.C.N., E.W., Z.M., and O.R.; Resources and Supervision, E.W., Z.M., and J.K.F.; Funding Acquisition, J.C.N., E.W., Z.M., J.K.F., and M.G.; Writing, J.C.N. and M.G.

## DECLARATION OF INTERESTS

The authors declare no competing interests.

Received: May 6, 2019  
Revised: January 6, 2020  
Accepted: May 5, 2020  
Published: June 4, 2020

## REFERENCES

1. Thompson, R.F., and Spencer, W.A. (1966). Habituation: a model phenomenon for the study of neuronal substrates of behavior. *Psychol. Rev.* 73, 16–43.
2. Rankin, C.H., Abrams, T., Barry, R.J., Bhatnagar, S., Clayton, D.F., Colombo, J., Coppola, G., Geyer, M.A., Glanzman, D.L., Marsland, S., et al. (2009). Habituation revisited: an updated and revised description of the behavioral characteristics of habituation. *Neurobiol. Learn. Mem.* 92, 135–138.
3. Epstein, L.H., Temple, J.L., Roemmich, J.N., and Bouton, M.E. (2009). Habituation as a determinant of human food intake. *Psychol. Rev.* 116, 384–407.
4. Thrailkill, E.A., Epstein, L.H., and Bouton, M.E. (2015). Effects of inter-food interval on the variety effect in an instrumental food-seeking task. Clarifying the role of habituation. *Appetite* 84, 43–53.
5. McSweeney, F.K., Murphy, E.S., and Kowal, B.P. (2005). Regulation of drug taking by sensitization and habituation. *Exp. Clin. Psychopharmacol.* 13, 163–184.
6. Grissom, N., and Bhatnagar, S. (2009). Habituation to repeated stress: get used to it. *Neurobiol. Learn. Mem.* 92, 215–224.
7. Ardiel, E.L., and Rankin, C.H. (2008). Behavioral plasticity in the *C. elegans* mechanosensory circuit. *J. Neurogenet.* 22, 239–255.
8. Pinsker, H., Kupfermann, I., Castellucci, V., and Kandel, E. (1970). Habituation and dishabituation of the gill-withdrawal reflex in aplysia. *Science* 167, 1740–1742.
9. Sinding, C., Valadier, F., Al-Hassani, V., Feron, G., Tromelin, A., Kontaris, I., and Hummel, T. (2017). New determinants of olfactory habituation. *Sci. Rep.* 7, 41047.
10. Koch, M. (1999). The neurobiology of startle. *Prog. Neurobiol.* 59, 107–128.
11. McDiarmid, T.A., Bernardos, A.C., and Rankin, C.H. (2017). Habituation is altered in neuropsychiatric disorders—a comprehensive review with

- recommendations for experimental design and analysis. *Neurosci. Biobehav. Rev.* **80**, 286–305.
12. Simons-Weidenmaier, N.S., Weber, M., Plappert, C.F., Pilz, P.K.D., and Schmid, S. (2006). Synaptic depression and short-term habituation are located in the sensory part of the mammalian startle pathway. *BMC Neurosci.* **7**, 38.
  13. Weber, M., Schnitzler, H.-U., and Schmid, S. (2002). Synaptic plasticity in the acoustic startle pathway: the neuronal basis for short-term habituation? *Eur. J. Neurosci.* **16**, 1325–1332.
  14. Marsden, K.C., and Granato, M. (2015). In vivo Ca(2+) imaging reveals that decreased dendritic excitability drives startle habituation. *Cell Rep.* **13**, 1733–1740.
  15. Glanzman, D.L. (2009). Habituation in aplysia: the Cheshire cat of neurobiology. *Neurobiol. Learn. Mem.* **92**, 147–154.
  16. Pilz, P.K.D., Carl, T.D., and Plappert, C.F. (2004). Habituation of the acoustic and the tactile startle responses in mice: two independent sensory processes. *Behav. Neurosci.* **118**, 975–983.
  17. Davis, M., and File, S.E. (1984). Intrinsic and extrinsic mechanisms of habituation and sensitization: Implications for the design and analysis of experiments. In *Habituation, Sensitization, and Behavior*, H.V.S. Peeke, and L.F. Petrinoich, eds. (Academic Press), pp. 287–323.
  18. Sugi, T., Ohtani, Y., Kumiya, Y., Igarashi, R., and Shirakawa, M. (2014). High-throughput optical quantification of mechanosensory habituation reveals neurons encoding memory in *Caenorhabditis elegans*. *Proc. Natl. Acad. Sci. USA* **111**, 17236–17241.
  19. Giles, A.C., Opperman, K.J., Rankin, C.H., and Grill, B. (2015). Developmental function of the PHR protein RPM-1 is required for learning in *Caenorhabditis elegans*. *G3* **5**, 2745–2757.
  20. Ardiel, E.L., McDiarmid, T.A., Timbers, T.A., Lee, K.C.Y., Safaei, J., Pelech, S.L., and Rankin, C.H. (2018). Insights into the roles of CMK-1 and OGT-1 in interstimulus interval-dependent habituation in *Caenorhabditis elegans*. *Proc. Biol. Sci.* **285**, 20182084.
  21. Ardiel, E.L., Yu, A.J., Giles, A.C., and Rankin, C.H. (2017). Habituation as an adaptive shift in response strategy mediated by neuropeptides. *NPJ Sci. Learn.* **2**, 9.
  22. Ardiel, E.L., Giles, A.C., Yu, A.J., Lindsay, T.H., Lockery, S.R., and Rankin, C.H. (2016). Dopamine receptor DOP-4 modulates habituation to repetitive photoactivation of a *C. elegans* polymodal nociceptor. *Learn. Mem.* **23**, 495–503.
  23. Crawley, O., Giles, A.C., Desbois, M., Kashyap, S., Birnbaum, R., and Grill, B. (2017). A MIG-15/JNK-1 MAP kinase cascade opposes RPM-1 signaling in synapse formation and learning. *PLoS Genet.* **13**, e1007095.
  24. Eddison, M., Belay, A.T., Sokolowski, M.B., and Heberlein, U. (2012). A genetic screen for olfactory habituation mutations in *Drosophila*: analysis of novel foraging alleles and an underlying neural circuit. *PLoS ONE* **7**, e51684.
  25. Wolf, F.W., Eddison, M., Lee, S., Cho, W., and Heberlein, U. (2007). GSK-3/Shaggy regulates olfactory habituation in *Drosophila*. *Proc. Natl. Acad. Sci. USA* **104**, 4653–4657.
  26. Rankin, C.H., and Wicks, S.R. (2000). Mutations of the *caenorhabditis elegans* brain-specific inorganic phosphate transporter *eat-4* affect habituation of the tap-withdrawal response without affecting the response itself. *J. Neurosci.* **20**, 4337–4344.
  27. Swierczek, N.A., Giles, A.C., Rankin, C.H., and Kerr, R.A. (2011). High-throughput behavioral analysis in *C. elegans*. *Nat. Methods* **8**, 592–598.
  28. Engel, J.E., and Wu, C.-F. (1996). Altered habituation of an identified escape circuit in *Drosophila* memory mutants. *J. Neurosci.* **16**, 3486–3499.
  29. Wolman, M.A., Jain, R.A., Marsden, K.C., Bell, H., Skinner, J., Hayer, K.E., Hogenesch, J.B., and Granato, M. (2015). A genome-wide screen identifies PAPP-AA-mediated IGFR signaling as a novel regulator of habituation learning. *Neuron* **85**, 1200–1211.
  30. Wolman, M.A., Jain, R.A., Liss, L., and Granato, M. (2011). Chemical modulation of memory formation in larval zebrafish. *Proc. Natl. Acad. Sci. USA* **108**, 15468–15473.
  31. Best, J.D., Berghmans, S., Hunt, J.J.F.G., Clarke, S.C., Fleming, A., Goldsmith, P., and Roach, A.G. (2008). Non-associative learning in larval zebrafish. *Neuropsychopharmacology* **33**, 1206–1215.
  32. Jain, R.A., Wolman, M.A., Marsden, K.C., Nelson, J.C., Shoenhard, H., Echeverry, F.A., Szi, C., Bell, H., Skinner, J., Cobbs, E.N., et al. (2018). A forward genetic screen in zebrafish identifies the G-protein-coupled receptor CaSR as a modulator of sensorimotor decision making. *Curr. Biol.* **28**, 1357–1369.e5.
  33. Marsden, K.C., Jain, R.A., Wolman, M.A., Echeverry, F.A., Nelson, J.C., Hayer, K.E., Miltenberg, B., Pereda, A.E., and Granato, M. (2018). A Cyfip2-dependent excitatory interneuron pathway establishes the innate startle threshold. *Cell Rep.* **23**, 878–887.
  34. Huang, K., Yanai, A., Kang, R., Arstikaitis, P., Singaraja, R.R., Metzler, M., Mullard, A., Haigh, B., Gauthier-Campbell, C., Gutekunst, C.-A., et al. (2004). Huntingtin-interacting protein HIP14 is a palmitoyl transferase involved in palmitoylation and trafficking of multiple neuronal proteins. *Neuron* **44**, 977–986.
  35. Labun, K., Montague, T.G., Gagnon, J.A., Thyme, S.B., and Valen, E. (2016). CHOPCHOP v2: a web tool for the next generation of CRISPR genome engineering. *Nucleic Acids Res.* **44** (W1), W272–W276.
  36. Hwang, W.Y., Fu, Y., Reyon, D., Maeder, M.L., Kaini, P., Sander, J.D., Joung, J.K., Peterson, R.T., and Yeh, J.-R.J. (2013). Heritable and precise zebrafish genome editing using a CRISPR-Cas system. *PLoS ONE* **8**, e68708.
  37. Davis, M., Gendelman, D.S., Tischler, M.D., and Gendelman, P.M. (1982). A primary acoustic startle circuit: lesion and stimulation studies. *J. Neurosci.* **2**, 791–805.
  38. Koyama, M., Kinkhabwala, A., Satou, C., Higashijima, S., and Fetcho, J. (2011). Mapping a sensory-motor network onto a structural and functional ground plan in the hindbrain. *Proc. Natl. Acad. Sci. USA* **108**, 1170–1175.
  39. Hale, M.E., Katz, H.R., Peek, M.Y., and Fremont, R.T. (2016). Neural circuits that drive startle behavior, with a focus on the Mauthner cells and spiral fiber neurons of fishes. *J. Neurogenet.* **30**, 89–100.
  40. Yao, C., Vanderpool, K.G., Delfiner, M., Eddy, V., Lucaci, A.G., Soto-Riveros, C., Yasumura, T., Rash, J.E., and Pereda, A.E. (2014). Electrical synaptic transmission in developing zebrafish: properties and molecular composition of gap junctions at a central auditory synapse. *J. Neurophysiol.* **112**, 2102–2113.
  41. Burgess, H.A., and Granato, M. (2007). Sensorimotor gating in larval zebrafish. *J. Neurosci.* **27**, 4984–4994.
  42. Kimmel, C.B., Eaton, R.C., and Powell, S.L. (1980). Decreased fast-start performance of zebrafish larvae lacking mauthner neurons. *J. Comp. Physiol.* **140**, 343–350.
  43. Singaraja, R.R., Hadano, S., Metzler, M., Givan, S., Wellington, C.L., Warby, S., Yanai, A., Gutekunst, C.-A., Leavitt, B.R., Yi, H., et al. (2002). HIP14, a novel ankyrin domain-containing protein, links huntingtin to intracellular trafficking and endocytosis. *Hum. Mol. Genet.* **11**, 2815–2828.
  44. Huang, K., Sanders, S., Singaraja, R., Orban, P., Cijssouw, T., Arstikaitis, P., Yanai, A., Hayden, M.R., and El-Husseini, A. (2009). Neuronal palmitoyl acyl transferases exhibit distinct substrate specificity. *FASEB J.* **23**, 2605–2615.
  45. Butland, S.L., Sanders, S.S., Schmidt, M.E., Riechers, S.-P., Lin, D.T.S., Martin, D.D.O., Vaid, K., Graham, R.K., Singaraja, R.R., Wanker, E.E., et al. (2014). The palmitoyl acyltransferase HIP14 shares a high proportion of interactors with huntingtin: implications for a role in the pathogenesis of Huntington's disease. *Hum. Mol. Genet.* **23**, 4142–4160.
  46. Singaraja, R.R., Huang, K., Sanders, S.S., Milnerwood, A.J., Hines, R., Lerch, J.P., Franciosi, S., Drisdell, R.C., Vaid, K., Young, F.B., et al. (2011). Altered palmitoylation and neuropathological deficits in mice lacking HIP14. *Hum. Mol. Genet.* **20**, 3899–3909.
  47. Kang, K.-H., and Bier, E. (2010). dHIP14-dependent palmitoylation promotes secretion of the BMP antagonist *Sog*. *Dev. Biol.* **346**, 1–10.
  48. Yanatori, I., Yasui, Y., Ouchi, K., and Kishi, F. (2015). Chlamydia pneumoniae CPJ0783 interaction with Huntingtin-protein14. *Int. Microbiol.* **18**, 225–233.

49. Ohyama, T., Verstreken, P., Ly, C.V., Rosenmund, T., Rajan, A., Tien, A.-C., Haueter, C., Schulze, K.L., and Bellen, H.J. (2007). Huntingtin-interacting protein 14, a palmitoyl transferase required for exocytosis and targeting of CSP to synaptic vesicles. *J. Cell Biol.* **179**, 1481–1496.
50. Rush, D.B., Leon, R.T., McCollum, M.H., Treu, R.W., and Wei, J. (2012). Palmitoylation and trafficking of GAD65 are impaired in a cellular model of Huntington's disease. *Biochem. J.* **442**, 39–48.
51. Skotte, N.H., Sanders, S.S., Singaraja, R.R., Ehrnhoefer, D.E., Vaid, K., Qiu, X., Kannan, S., Verma, C., and Hayden, M.R. (2017). Palmitoylation of caspase-6 by HIP14 regulates its activation. *Cell Death Differ.* **24**, 433–444.
52. Lemonidis, K., MacLeod, R., Baillie, G.S., and Chamberlain, L.H. (2017). Peptide array-based screening reveals a large number of proteins interacting with the ankyrin-repeat domain of the zDHHC17 S-acyltransferase. *J. Biol. Chem.* **292**, 17190–17202.
53. Wolman, M.A., de Groh, E.D., McBride, S.M., Jongens, T.A., Granato, M., and Epstein, J.A. (2014). Modulation of cAMP and ras signaling pathways improves distinct behavioral deficits in a zebrafish model of neurofibromatosis type 1. *Cell Rep.* **8**, 1265–1270.
54. Tanouye, M.A., Ferrus, A., and Fujita, S.C. (1981). Abnormal action potentials associated with the Shaker complex locus of *Drosophila*. *Proc. Natl. Acad. Sci. USA* **78**, 6548–6552.
55. Brew, H.M., Hallows, J.L., and Tempel, B.L. (2003). Hyperexcitability and reduced low threshold potassium currents in auditory neurons of mice lacking the channel subunit Kv1.1. *J. Physiol.* **548**, 1–20.
56. Lee, J., Ueda, A., and Wu, C.-F. (2008). Pre- and post-synaptic mechanisms of synaptic strength homeostasis revealed by slowpoke and shaker K<sup>+</sup> channel mutations in *Drosophila*. *Neuroscience* **154**, 1283–1296.
57. Kaplan, W.D., and Trout, W.E., 3rd. (1969). The behavior of four neurological mutants of *Drosophila*. *Genetics* **61**, 399–409.
58. Smart, S.L., Lopantsev, V., Zhang, C.L., Robbins, C.A., Wang, H., Chiu, S.Y., Schwartzkroin, P.A., Messing, A., and Tempel, B.L. (1998). Deletion of the K(V)1.1 potassium channel causes epilepsy in mice. *Neuron* **20**, 809–819.
59. Yin, X.-M., Lin, J.-H., Cao, L., Zhang, T.-M., Zeng, S., Zhang, K.-L., Tian, W.-T., Hu, Z.-M., Li, N., Wang, J.-L., et al. (2018). Familial paroxysmal kinesigenic dyskinesia is associated with mutations in the KCNA1 gene. *Hum. Mol. Genet.* **27**, 625–637.
60. Gubitosi-Klug, R.A., Mancuso, D.J., and Gross, R.W. (2005). The human Kv1.1 channel is palmitoylated, modulating voltage sensing: Identification of a palmitoylation consensus sequence. *Proc. Natl. Acad. Sci. USA* **102**, 5964–5968.
61. Wan, J., Roth, A.F., Bailey, A.O., and Davis, N.G. (2007). Palmitoylated proteins: purification and identification. *Nat. Protoc.* **2**, 1573–1584.
62. Globa, A.K., and Bamji, S.X. (2017). Protein palmitoylation in the development and plasticity of neuronal connections. *Curr. Opin. Neurobiol.* **45**, 210–220.
63. Brewster, D.L., and Ali, D.W. (2013). Expression of the voltage-gated potassium channel subunit Kv1.1 in embryonic zebrafish Mauthner cells. *Neurosci. Lett.* **539**, 54–59.
64. Watanabe, T., Shimazaki, T., Mishiro, A., Suzuki, T., Hirata, H., Tanimoto, M., and Oda, Y. (2014). Coexpression of auxiliary Kvβ2 subunits with Kv1.1 channels is required for developmental acquisition of unique firing properties of zebrafish Mauthner cells. *J. Neurophysiol.* **111**, 1153–1164.
65. Kimmel, C.B., Sessions, S.K., and Kimmel, R.J. (1981). Morphogenesis and synaptogenesis of the zebrafish Mauthner neuron. *J. Comp. Neurol.* **198**, 101–120.
66. Lacoste, A.M.B., Schoppik, D., Robson, D.N., Haesemeyer, M., Portugues, R., Li, J.M., Randlett, O., Wee, C.L., Engert, F., and Schier, A.F. (2015). A convergent and essential interneuron pathway for Mauthner-cell-mediated escapes. *Curr. Biol.* **25**, 1526–1534.
67. Stowers, R.S., and Isacoff, E.Y. (2007). *Drosophila* huntingtin-interacting protein 14 is a presynaptic protein required for photoreceptor synaptic transmission and expression of the palmitoylated proteins synaptosome-associated protein 25 and cysteine string protein. *J. Neurosci.* **27**, 12874–12883.
68. Eaton, R.C., Farley, R.D., Kimmel, C.B., and Schabtach, E. (1977). Functional development in the Mauthner cell system of embryos and larvae of the zebra fish. *J. Neurobiol.* **8**, 151–172.
69. Noritake, J., Fukata, Y., Iwanaga, T., Hosomi, N., Tsutsumi, R., Matsuda, N., Tani, H., Iwanari, H., Mochizuki, Y., Kodama, T., et al. (2009). Mobile DHHC palmitoylating enzyme mediates activity-sensitive synaptic targeting of PSD-95. *J. Cell Biol.* **186**, 147–160.
70. Kang, R., Wan, J., Arstikaitis, P., Takahashi, H., Huang, K., Bailey, A.O., Thompson, J.X., Roth, A.F., Drisdell, R.C., Mastro, R., et al. (2008). Neural palmitoyl-proteomics reveals dynamic synaptic palmitoylation. *Nature* **456**, 904–909.
71. Misra, C., Restituito, S., Ferreira, J., Rameau, G.A., Fu, J., and Ziff, E.B. (2010). Regulation of synaptic structure and function by palmitoylated AMPA receptor binding protein. *Mol. Cell. Neurosci.* **43**, 341–352.
72. Brigidi, G.S., Sun, Y., Beccano-Kelly, D., Pitman, K., Mobasser, M., Borgland, S.L., Milnerwood, A.J., and Bamji, S.X. (2014). Palmitoylation of δ-catenin by DHHC5 mediates activity-induced synapse plasticity. *Nat. Neurosci.* **17**, 522–532.
73. Keith, D.J., Sanderson, J.L., Gibson, E.S., Woolfrey, K.M., Robertson, H.R., Olszewski, K., Kang, R., El-Husseini, A., and Dell'acqua, M.L. (2012). Palmitoylation of A-kinase anchoring protein 79/150 regulates dendritic endosomal targeting and synaptic plasticity mechanisms. *J. Neurosci.* **32**, 7119–7136.
74. Milnerwood, A.J., Parsons, M.P., Young, F.B., Singaraja, R.R., Franciosi, S., Volta, M., Bergeron, S., Hayden, M.R., and Raymond, L.A. (2013). Memory and synaptic deficits in Hip14/DHHC17 knockout mice. *Proc. Natl. Acad. Sci. USA* **110**, 20296–20301.
75. Sanders, S.S., Parsons, M.P., Mui, K.K.N., Southwell, A.L., Franciosi, S., Cheung, D., Waltl, S., Raymond, L.A., and Hayden, M.R. (2016). Sudden death due to paralysis and synaptic and behavioral deficits when Hip14/Zdhhc17 is deleted in adult mice. *BMC Biol.* **14**, 108.
76. Engel, J.E., and Wu, C.-F. (1998). Genetic dissection of functional contributions of specific potassium channel subunits in habituation of an escape circuit in *Drosophila*. *J. Neurosci.* **18**, 2254–2267.
77. Joiner, M.A., Asztalos, Z., Jones, C.J., Tully, T., and Wu, C.-F. (2007). Effects of mutant *Drosophila* K<sup>+</sup> channel subunits on habituation of the olfactory jump response. *J. Neurogenet.* **21**, 45–58.
78. Pujol-Martí, J., Zecca, A., Baudoin, J.-P., Faucherre, A., Asakawa, K., Kawakami, K., and López-Schier, H. (2012). Neuronal birth order identifies a dimorphic sensorineural map. *J. Neurosci.* **32**, 2976–2987.
79. Lakhina, V., Marcaccio, C.L., Shao, X., Lush, M.E., Jain, R.A., Fujimoto, E., Bonkowsky, J.L., Granato, M., and Raper, J.A. (2012). Netrin/DCC signaling guides olfactory sensory axons to their correct location in the olfactory bulb. *J. Neurosci.* **32**, 4440–4456.
80. Yamanaka, I., Miki, M., Asakawa, K., Kawakami, K., Oda, Y., and Hirata, H. (2013). Glycinergic transmission and postsynaptic activation of CaMKII are required for glycine receptor clustering in vivo. *Genes Cells* **18**, 211–224.
81. Neff, M.M., Turk, E., and Kalishman, M. (2002). Web-based primer design for single nucleotide polymorphism analysis. *Trends Genet.* **18**, 613–615.
82. Thermes, V., Grabher, C., Ristoratore, F., Bourrat, F., Choulika, A., Wittbrodt, J., and Joly, J.-S. (2002). I-SceI meganuclease mediates highly efficient transgenesis in fish. *Mech. Dev.* **118**, 91–98.
83. Ikeda, H., Delargy, A.H., Yokogawa, T., Urban, J.M., Burgess, H.A., and Ono, F. (2013). Intrinsic properties of larval zebrafish neurons in ethanol. *PLoS ONE* **8**, e63318.
84. Randlett, O., Wee, C.L., Naumann, E.A., Nnaemeka, O., Schoppik, D., Fitzgerald, J.E., Portugues, R., Lacoste, A.M.B., Riegler, C., Engert, F., and Schier, A.F. (2015). Whole-brain activity mapping onto a zebrafish brain atlas. *Nat. Methods* **12**, 1039–1046.

**STAR★METHODS**

**KEY RESOURCES TABLE**

REAGENT or RESOURCE	SOURCE	IDENTIFIER
<b>Antibodies</b>		
Rabbit anti-Kv1.1	Sigma	Cat# AB5174; RRID: AB_91720
Chicken anti-GFP	Aves Labs	Cat # GFP-120; RRID: AB_2307313
Alexa 488 Donkey anti-Chicken	Jackson ImmunoResearch	RRID: AB_2340375
Alexa-633 Goat anti-Rabbit	Invitrogen	RRID: AB_2535731
Rabbit anti-Flag	Sigma	Cat # F7425; RRID: AB_439687
Rabbit anti-HA	Cell Signaling	Cat # C29F4; RRID: AB_10693385
Donkey anti-Rabbit HRP	GE Amersham	Cat# NA934; RRID: AB_772206
<b>Chemicals, Peptides, and Recombinant Proteins</b>		
Cas9 Protein	PNA Bio	Cat# CP02
Rolipram	Sigma	Cat# R6520
SC79	Sigma	Cat# 0749
U0126	Cell Signaling	Cat# 9903S
<b>Experimental Models: Organisms/Strains</b>		
Zebrafish: <i>Tg(hsp70:GAL4FFDMC)130a; Tg(UAS:gap43-citrine)</i>	[78, 79]	ZFIN: ZDB-ALT-120320-6; ZFIN: ZDB-FISH-150901-21649
Zebrafish: <i>Tg(hsp70GFF62A); Tg(UAS:gcamp6s)</i>	[14, 80]	ZFIN: ZDB-ALT-150717-1; ZFIN: ZDB-TGCONSTRUCT-160316-3
Zebrafish: <i>Tg(-6.7FRhctR:gal4VP16); Tg(UAS:GCaMP5)</i>	[66]	ZFIN: ZDB-TGCONSTRUCT-151028-8; ZFIN: ZDB-ALT-151028-4
Zebrafish: <i>slow learner / hip14<sup>p174</sup></i>	[29]	ZFIN: ZDB-ALT-150701-4
Zebrafish: <i>fool me twice / kcna1a<sup>p181</sup></i>	[29]	ZFIN: ZDB-ALT-150701-11
Zebrafish: <i>hip14<sup>p408</sup></i>	This study	ZFIN: ZDB-ALT-181106-7
Zebrafish: <i>kcna1a<sup>p410</sup></i>	This study	ZFIN: ZDB-ALT-181106-9
Zebrafish: <i>Tg(hsp70:hip14-p2a-mKate)</i>	This study	ZFIN: ZDB-ALT-181106-8
<b>Oligonucleotides</b>		
Oligonucleotides for genotyping, generating CRISPR mutations, and cloning can be found in <a href="#">Table S1</a> .	N/A	N/A
<b>Recombinant DNA</b>		
pDR274-Hip14-sgRNA-7	This study	N/A
pCHK-hip14-HA	This study	N/A
pCHK-hip14-DHHS-HA	This study	N/A
pCHK-kcna1a-FLAG	This study	N/A
pCHK-kcna1a-N250K-FLAG	This study	N/A
pCHK-kcna1a-C238A-FLAG	This study	N/A
pRIES2-AcGFP-kcna1a	This study	N/A
pRIES2-AcGFP-kcna1a-N250K	This study	N/A
pRIES2-AcGFP-kcna1a-C238A	This study	N/A
pENTR-hip14-p2a-mKate	This study	N/A
pDEST-hsp70-hip14-p2a-mKate	This study	N/A
<b>Software and Algorithms</b>		
ChopChop v2	[36]	<a href="https://chopchop.cbu.uib.no/">https://chopchop.cbu.uib.no/</a>
GraphPad Prism	GraphPad Software	<a href="https://www.graphpad.com/">https://www.graphpad.com/</a>

(Continued on next page)

### Continued

REAGENT or RESOURCE	SOURCE	IDENTIFIER
dCAPS	[81]	<a href="http://helix.wustl.edu/dcaps/dcaps.html">http://helix.wustl.edu/dcaps/dcaps.html</a>
FLOTE & DAQTimer	[42]	<a href="https://science.nichd.nih.gov/confluence/display/burgess/Software">https://science.nichd.nih.gov/confluence/display/burgess/Software</a>
Other		
35mm glass-bottomed Petri dishes with 10mm Microwell	MatTek	P35G-0-10-C

## RESOURCE AVAILABILITY

### Lead Contact

Dr. Michael Granato ([granatom@pennmedicine.upenn.edu](mailto:granatom@pennmedicine.upenn.edu)).

### Materials Availability

Additional information and requests for resources and reagents should be directed to the Lead Contact, Dr. Michael Granato ([granatom@pennmedicine.upenn.edu](mailto:granatom@pennmedicine.upenn.edu)).

### Data and Code Availability

This study did not generate datasets/code.

## EXPERIMENTAL MODEL AND SUBJECT DETAILS

All animal protocols were approved by the University of Pennsylvania Institutional Animal Care and Use Committee (IACUC).

Mutant alleles were generated using CRISPR-Cas9 as previously described [32]. sgRNA were designed using ChopChop v2 [35], oligos were annealed and directly ligated into pDR274 [36]. sgRNA were then synthesized using the T7 MEGAshortscript kit (Ambion) and purified using the MEGAclean kit (Ambion). Cas9 protein (PNA Bio) and sgRNAs were mixed and injected into 1-cell stage TLF embryos. G<sub>0</sub> injected larvae were raised and outcrossed to identify and establish heterozygous carrier lines.

To generate *Tg(hsp70-hip14-p2a-mKate)*, Gateway cloning was employed to combine *hip14-p2a-mKate* into a pDest vector containing the *hsp70* promoter and I-sce1 restriction sites. I-sce1 transgenesis was performed as previously described [82] in 1-cell stage embryos from *hip14+/-* incrosses. Transgenic lines were identified as previously described [33]. Briefly, 24 hpf F<sub>1</sub> offspring of G<sub>0</sub>-injected fish were placed into Eppendorf tubes and incubated at 37°C for 30 min, recovered in Petri dishes for 60 min, and screened for mKate with a fluorescent stereomicroscope (Olympus MVX10).

Fish carrying the gal4 drivers *Tg(GFFDMC130A)* and *Tg(GFF62A)* were provided by Dr. Koichi Kawakami [78, 80]. *Tg(UAS:gap43-citrine)* fish were provided by Dr. Jonathan Raper [79]. Fish carrying the gal4 driver *Tg(-6.7FRhcrR:gal4VP16)* and *Tg:UAS:GCaMP5* were provided by Dr. David Schoppik.

Adult zebrafish and embryos were raised at 29°C on a 14-h:10-h light:dark cycle.

*hip14* and *kcna1a* mutations *p174* and *p181* were genotyped using proprietary allele specific primer sequences (LGC Genomics) and the KASP assay method, which utilizes FRET to distinguish between alleles. For genotyping in the context of *Tg(hsp70-hip14-p2a-mKate)* we developed a dCAPS assay using the dCAPS program (<http://helix.wustl.edu/dcaps/dcaps.html>) to design appropriate primers, with the reverse primer binding in the intron adjacent to the mutation [81]. Alleles *p408* and *p410* were also genotyped using dCAPS PCR genotyping.

## METHOD DETAILS

### Behavior Testing

Behavioral experiments were performed on 4–5 dpf larvae and behavior was analyzed using FLOTE software as previously described [30, 41]. Larvae were arrayed in a laser-cut 36-well acrylic dish attached via an aluminum rod to a vibrational exciter (4810; Brüel and Kjær, Norcross, GA), which delivered acoustic vibrational stimuli (2ms duration, 1000 Hz waveforms). For habituation assay, 10 stimuli were delivered with a 20 s ISI, followed by 30 stimuli with a 1 s ISI. Habituation was calculated as: % Habituation = (1-[response frequency Stimuli 21–30] ÷ [response frequency baseline])\*100. For startle sensitivity assay, 60 stimuli (10 trials for each of the following stimuli: 4.6 dB, 13.5 dB, 17.2 dB, 20.7 dB, 23.9 dB, 25.9 dB) were delivered with a 20 s ISI. Sensitivity index for each animal was calculated by measuring the area under the curve of acoustic startle frequency versus stimulus intensity using GraphPad Prism. Acoustic startles were identified using defined kinematic parameters (latency, turn angle, duration and maximum angular velocity).

For habituation and acoustic startle sensitivity assays, behavior was recorded at 1000 frames per second using a Photron UX50 camera suspended above the dish. For spontaneous movement assays, no stimuli were delivered; behavior was recorded for 3 minutes at 50 frames per second.

### WGS and Molecular Cloning of *hip14* and *kcna1a*

Positional cloning to identify the location of the learning deficit-associated *p174* and *p181* mutant alleles was performed as previously described [29, 32]. Briefly, pools of 50 behaviorally identified *p174* and *p181* mutant larvae were made and genomic DNA (gDNA) libraries were created. gDNA was sequenced with 100-bp paired-end reads on the Illumina HiSeq 2000 platform, and homozygosity analysis was done using 463,379 SNP markers identified by sequencing gDNA from ENU-mutagenized TLF and WIK males as described previously [29].

### Ca<sup>2+</sup> Imaging

Combined Ca<sup>2+</sup> imaging and acoustic startle experiments were performed as described previously [14]. Larvae were head-fixed in glass-bottomed Petri dishes (35mm Petri dish, 10mm Microwell P35G-0-10-C; MatTek) with 2% low-melt agarose diluted in bath solution containing 112mM NaCl, 5mM HEPES pH 7.5, 2mM CaCl<sub>2</sub>, 3mM glucose, 2mM KCl, 1mM MgCl<sub>2</sub> [83]. Tails were freed to permit behavioral responses to tap stimuli, and dishes were filled halfway with bath solution. 5-6 baseline responses were obtained by delivering acoustic tap stimuli every 2 minutes using a stage-mounted speaker. Short term habituation was then induced by delivering 25 tap stimuli with a 5 s interstimulus interval. Ca<sup>2+</sup> transients were captured using a spinning disk confocal microscope, while behavioral responses were recorded at 500fps using a camera suspended above the larva. For lateral dendrite analysis during habituation,  $\Delta F/F_0$  values were normalized to account for indicator sensitivity-related decreases in soma activity during action potentials as previously described [14].

### Pharmacology

SC79 (Sigma #0749), U0126 (Cell Signaling Technology #9903S), and rolipram (Sigma #R6520) were dissolved in 100% DMSO and administered at a final concentration of 1% DMSO. SC79 and U0126 were administered at a final concentration of 1  $\mu$ M; rolipram was administered at a final concentration of 10  $\mu$ M. All compounds were administered for 30 minutes prior to testing with the exception of SC79, which was administered chronically as previously described [29] (replacing media daily from 3-5dpf).

To generate drug stocks: 5mg of SC79 was diluted in 1mL DMSO to produce a 13.7mM stock solution; 73  $\mu$ L of this solution was then diluted in 10mL DMSO to produce a 100  $\mu$ M (100x) stock. 5mg of U0126 was diluted in 1.3mL of DMSO to produce a 10mM solution. This solution was then diluted 1:100 in DMSO to produce a 100  $\mu$ M (100x) stock solution. 2.5mg of rolipram was diluted in 9mL DMSO to produce a 1mM (100x) stock solution.

### Electrophysiology in N2a cells

All recordings were performed at room temperature (20 - 21°C). Data were acquired with an Axopatch 200B amplifier at 5 kHz. Currents were filtered by an eight-pole Bessel filter at 1 kHz and sampled at 5 kHz with an 18-bit A/D converter. Electrode capacitance was compensated electronically, and 60% of series resistance was compensated with a lag of 10  $\mu$ s. Electrodes were made from thick-walled PG10150-4 glass (World Precision Instruments). HEKA Pulse software (HEKA Elektronik, Germany) was used for data acquisition and stimulation protocols. Igor Pro was used for graphing and data analysis (WaveMetrics). Leak subtractions were not applied in the current study.

The N2a mouse neuroblastoma cell line was cultured in Eagle's minimum essential medium supplemented with 10% FBS and 0.5  $\times$  penicillin/streptomycin (Invitrogen) at 37°C in a humidified incubator with 5% CO<sub>2</sub>. Whole-cell currents were recorded in N2a cells 48 hours after transfection. The pipette solution contained (in mM): 140 K<sup>+</sup>, 1 Mg<sup>2+</sup>, 1 Ca<sup>2+</sup>, 30 Cl<sup>-</sup>, 11 EGTA and 10 HEPES, pH 7.3 adjusted by methanesulfonic acid, :300 mOsm. The bath solution contained (in mM): 150 Na<sup>+</sup>, 5.4 K<sup>+</sup>, 1.5 Ca<sup>2+</sup>, 1 Mg<sup>2+</sup>, 150 Cl<sup>-</sup>, 20 glucose, 1  $\mu$ M TTX, and 10 HEPES, pH 7.4 adjusted by methanesulfonate, :320 mOsm. The tip size of the electrode filled with the pipette solution was estimated as having a resistance of 1.5-3 M $\Omega$  in the bath solution before cell contact. Whole-cell patch clamp resistance was > 1 G $\Omega$  during whole-cell recording experiments.

### ABE Palmitoylation Assays

HEK293 cells were transiently transfected with 1 $\mu$ g total of DNA using Mirus LT1 transfection reagent. The ABE assays were performed 15 hours after transfection as previously described [61].

### Immunohistochemistry

*Tg:(UAS:gap43:Citrine)* was expressed under the control of the gal4 driver *Tg:(GFFDMC130a)*. Animals were fixed in 4% Paraformaldehyde and 0.25% Triton (PBT). To label the spiral fiber terminals, *Tg:UAS:GCaMP5* was expressed under the control of the gal4 driver *Tg:(-6.7FRhcrtr:gal4VP16)*. Fish were stained as previously described [84]. Larvae were washed in PBT and then incubated in 150 mM Tris-HCl, pH 9 for 5 minutes at room temperature. Larvae were then shifted to 70°C for 15 minutes, washed with PBT, and permeabilized in 0.05% Trypsin-EDTA for 45 minutes on ice. Larvae were then washed with PBT, blocked with PBT + 1% bovine serum albumin + 2% normal goat serum + 1% DMSO, and then incubated for 48 hours (as previously described [63]) at 4°C with rocking in blocking solution containing antibodies against GFP (1:500 Chicken anti-GFP Aves Labs, #GFP-120) and Kv1.1 (1:200

Rabbit anti-Kv1.1; Sigma, #AB5174). Samples were then washed in PBT and incubated overnight at 4°C with rocking in secondary antibodies diluted in block solution. Larval jaws were dissected away, and fish mounted ventral side up in Vectashield. 1024x1024 resolution stacks were then collected with an inverted confocal microscope (Zeiss LSM880), using a 63x water immersion objective. Fiji was used to quantify Kv1.1 or GCaMP5 signal blind to genotype. Sum projections were generated for the confocal slices encompassing the Mauthner axon initial segment. Regions of interest were drawn over the Mauthner AIS segment from the medial extent of the soma to the point at which the axon begins its posterior turn, extending anteriorly and posteriorly to encompass a region of approximately the same width as the Mauthner soma. (In the context of spiral fiber labeling via the gal4 driver *Tg(-6.7FRhcrTR:gal4VP16)*, regions of interest were drawn around the GCaMP5 labeled spiral fiber axon terminals.) Total fluorescence intensity in the Kv1.1 or GCaMP5 channel within these regions of interest was then calculated and divided by the area of the ROI.

### Heat Shock-Induced *hip14* Rescue

To induce expression of *Hip14-p2a-mKate*, 4- or 5-dpf larvae were arrayed in individual wells of a 96-well plate and placed at 37°C for 40 min in a thermocycler. Larvae were then placed in Petri dishes and allowed to recover for 140 minutes in the 5dpf condition (or 1 day in the 4dpf condition). Importantly, the transgene had no effect on habituation learning under normal temperature raising conditions (28°C) indicating that *hip14* expression is dependent on heat-shock.

### QUANTIFICATION AND STATISTICAL ANALYSIS

Statistical analyses, including calculation of means, SD and SE, were performed using Prism (GraphPad). D'Agostino & Pearson normality test was used to test whether data values were normally distributed. In the case of normal distribution, significance was assessed using t tests or ANOVA with Tukey's post hoc test for multiple comparisons as indicated. If data were not normally distributed, Kruskal-Wallis test with Dunn's multiple comparisons was used.